Supporting Information

Tuning Allostery through integration of Disorder-to-order with a Residue Network

Jingheng Wang[1§], Riya Samanta[2§], Gregory Custer[3], Christopher Look[3], Silvina Matysiak[3] & Dorothy Beckett[1*],

[1]Department of Chemistry & Biochemistry, University of Maryland, College Park, MD 20742
[2]Biophysics Graduate Program, University of Maryland, College Park, MD 20742
[3]Fischell Department of Bioengineering, University of Maryland, College Park, MD 20742

*Corresponding author: email dbeckett@umd.edu

Simulation Setup

For each simulation, the protein was placed in a rhombic dodecahedral box with boundaries extending out ~1 nm from the protein. The system was then solvated with ~20300 SPC/E water molecules.[1] Random replacement of a water molecule with a Na^+ counterion rendered the system neutral. Prior to each production run, the energy of the system was minimized using the steepest descent method. After minimization, NVT and NPT equilibration runs, each of 100 ps, were carried out using position restraints with a force constant of 1000 kJ mol^{-1} nm^{-2} on the protein and ligand. Position restraints were removed for the production run, which used an NPT ensemble at a temperature of 300 K and a pressure of 1 bar. As our previous work indicated that the simulations take no longer than 500 ns to equilibrate,[2] the duration of the production run was 1 μs, with the final 500 ns used for analysis.

The GROMACS 4.6 simulator [3-5] with the OPLS-AA force field [6] was used for simulation. Parameters for btnOH-AMP were identical to those used in our previous publications and are available upon request.[17] The time step for the simulations was 2 fs, with updating of neighbor lists every five steps. The LINCS algorithm was used to constrain bond lengths. Protein/ligand and water/ion temperature were regulated independently using the V-rescale algorithm [7] with a time constant of 0.1 ps. The ligand was grouped with the protein for temperature coupling while the Na^+ counterion was grouped with water. The Parrinello-Rahman barostat [8] was used for isotropic pressure coupling, with a time constant of 2 ps and a compressibility of 4.5×10^{-5} bar^{-1}.

Circular dichroism (CD) spectroscopy

The CD spectra were acquired by a JASCO J-810 (JASCO) spectrophotometer equipped with a Peltier temperature control unit. All spectra were collected using a 2mm pathlength quartz cuvette at 20°C. Data were recorded at 1nm intervals from 260 to 200nm at a scan speed of 50nm/min and a bandwidth of 1nm. To minimize the signal background from salt, spectra for the majority of the BirA variants were acquired in low salt Standard Buffer (10mM Tris, 50mM KCl, 2.5mM $MgCl_2$, pH=7.5 at 20°C). Due to its limited solubility in 50 mM KCl, spectra for the

BirA^{E313A} variant were acquired Standard Buffer containing 200mM KCl. Each final spectrum is the average of three measurements.

Table S1. Proton Release Linked to Effector Binding to BirA

Buffering agent	ΔH^{o}_{app} (kcal/mol)		
	WT	K172A	Y178C
Bistris	-10.6±0.2	-12.1±0.1	-11.8±0.1
MES	-10.1±0.2	-11.6±0.1	-10.2±0.1
Citrate	-9.4±0.1	-11.2±0.1	-9.7±0.2
n_{H+}	-0.166±0.005	-0.12±0.02	-0.35±0.07

Measurements were performed at 20^{o}C, pH 6.0 in Standard Buffer containing the appropriate buffering agent at 10 mM concentration. The reported errors were propagated from results of at least two independent TAPS measurements. The number of protons released was obtained from linear regression of the data using Equation 1.

Table S2: Gibbs free energies of bio-5'-AMP binding and dimerization for variants subjected to Force Distribution Analysis

BirA variant	$\Delta G^{o}_{bio\text{-}5'\text{-}AMP}$ (kcal/mol)[a]	ΔG^{o}_{DIM} (kcal/mol)[a]
wt	-13.8±0.2	-6.4±0.2
M211A	-11.58±0.09	-5.2±0.2
P143A	-13.5±0.2	-5.5±0.2
P143A/M211A	-12.0±0.1	-4.0±0.2

a. Values were previously reported.[2]

Table S3. Variants Show Punctual Stress Changes for Residues in that Helix the Contributes to BirA Dimerization

Residue	Variant			Nonbonded Partner/Interaction
	M211A	P143A	P143A/M211A	
G142		788±102	941±40	Disorder to order transition
P143		1010±113	1032±49	
A144		266±100	203±53	
A145		396±86		
A146			445±28	
I147		168±78	262±32	
G148		244±50		
L149				
S150		423±79		N175, Hydrogen Bond
L151				
V152		196±73	257±48	F253, Hydrophobic
I153			214±124	
G154				
I155		157±79		W265, Hydrophobic
V156	182±78	201±71	230±60	L246 Hydrophobic
M157				
A158				
E159	321±117	198±130	261±163	R264 Electrostatic
V160				
L161		198±95	289±96	G165 Hydrogen Bond
R162		582±189	389±198	D167 (BB) K168(BB) V169 (BB) Charged Hydrogen Bonds
K163		223±176		E245 Electrostatic
L164				
G165				
A166	344±187	216±185	281±205	A229 Hydrophobic
D167(BB)		580±186		R162 Charged Hydrogen Bond
K168(BB)		206±86		R162 Charged Hydrogen Bonds
V169(BB)		289±167		R162 Charged Hydrogen Bonds

The color code is the same as that used to illustrate the residues with significant punctual stress differences in Figure 5.

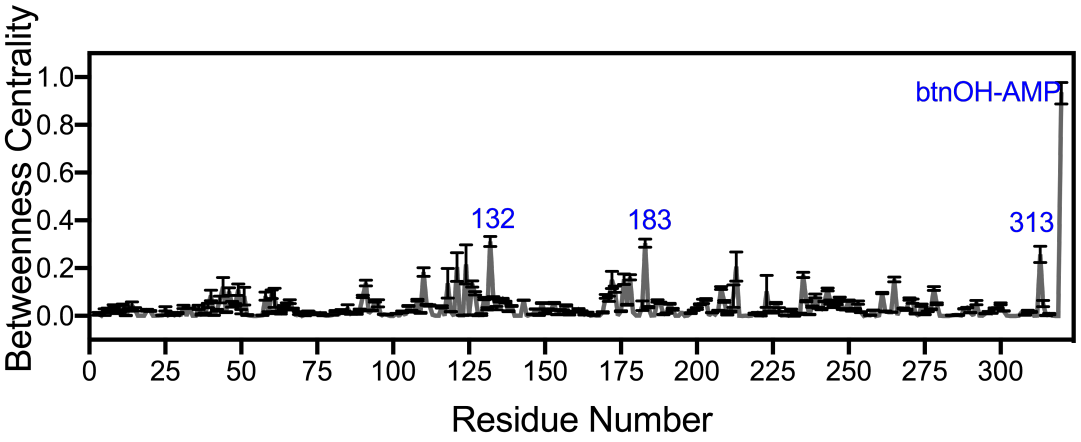

Figure S1. Betweenness Centrality values for BirA residues relative to those calculated for btnOH-AMP normalized to one.

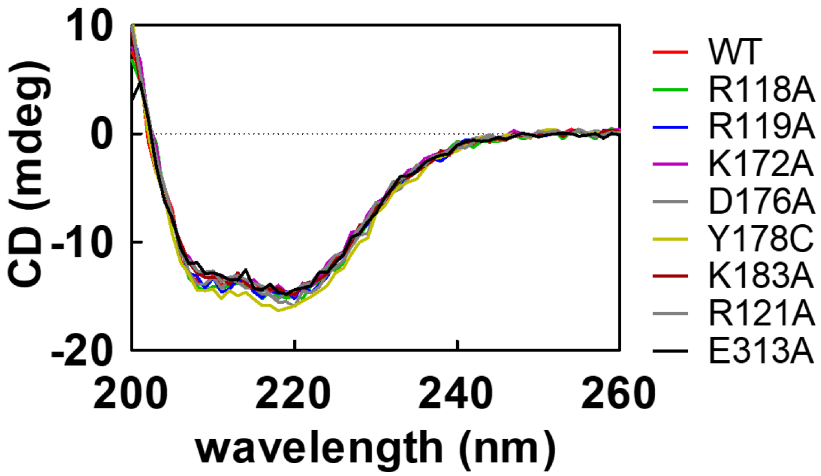

Figure S2. CD Spectra for all variants are similar to that of BirA^{wt}. Spectra are the average of three measurements. Spectra were acquired at 20^{o}C in Standard Buffer containing 50mM KCl for all variants except for that of BirA,^{E313A} which was acquired in 200 mM KCl due to its tendency to precipitate at the lower salt concentration.

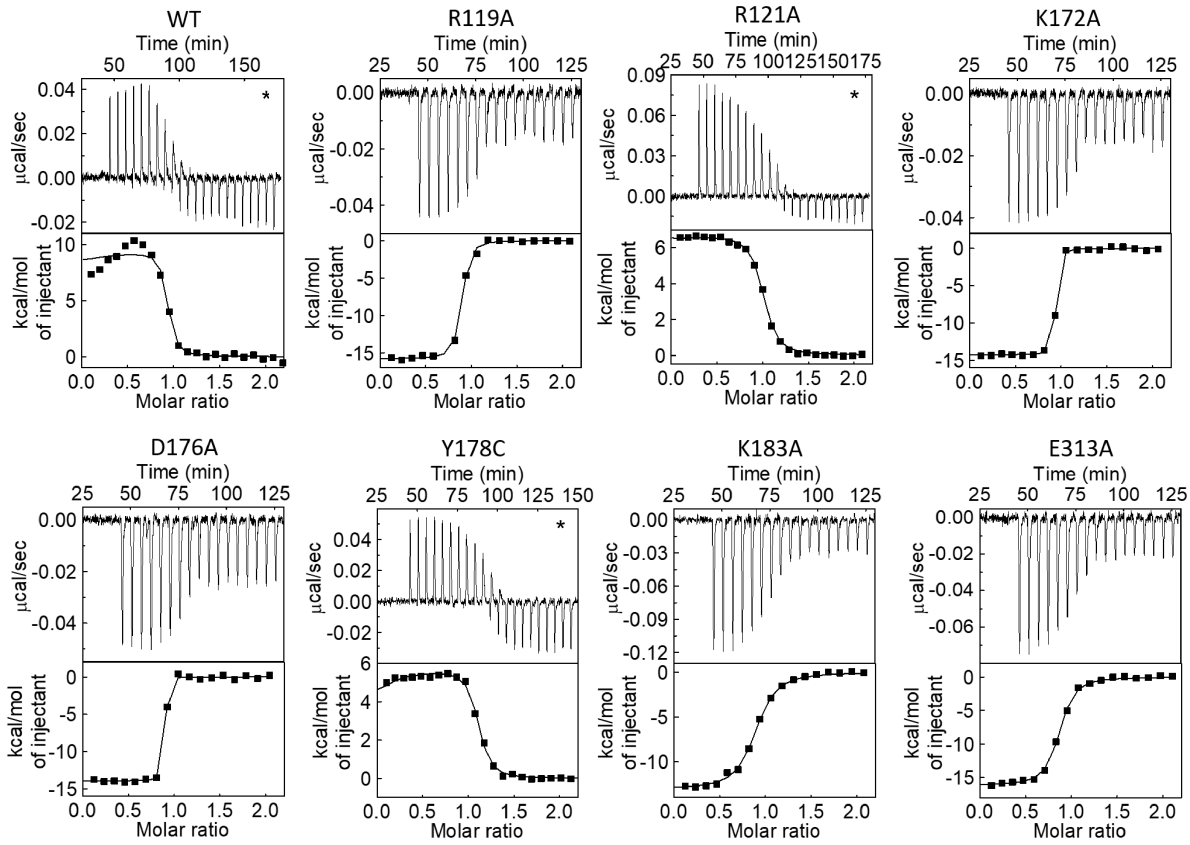

Figure S3. ITC measurements of bio-5'-AMP binding to BirA variants. For each variant the top panel shows the thermogram (adjusted for the baseline) and the bottom panel shows the binding isotherm and best-fit curves to a single-site or competitive binding model. Direct titrations show negative heat signals and displacement titrations, with asterisks, show positive heat signals in the first injections of the thermograms.

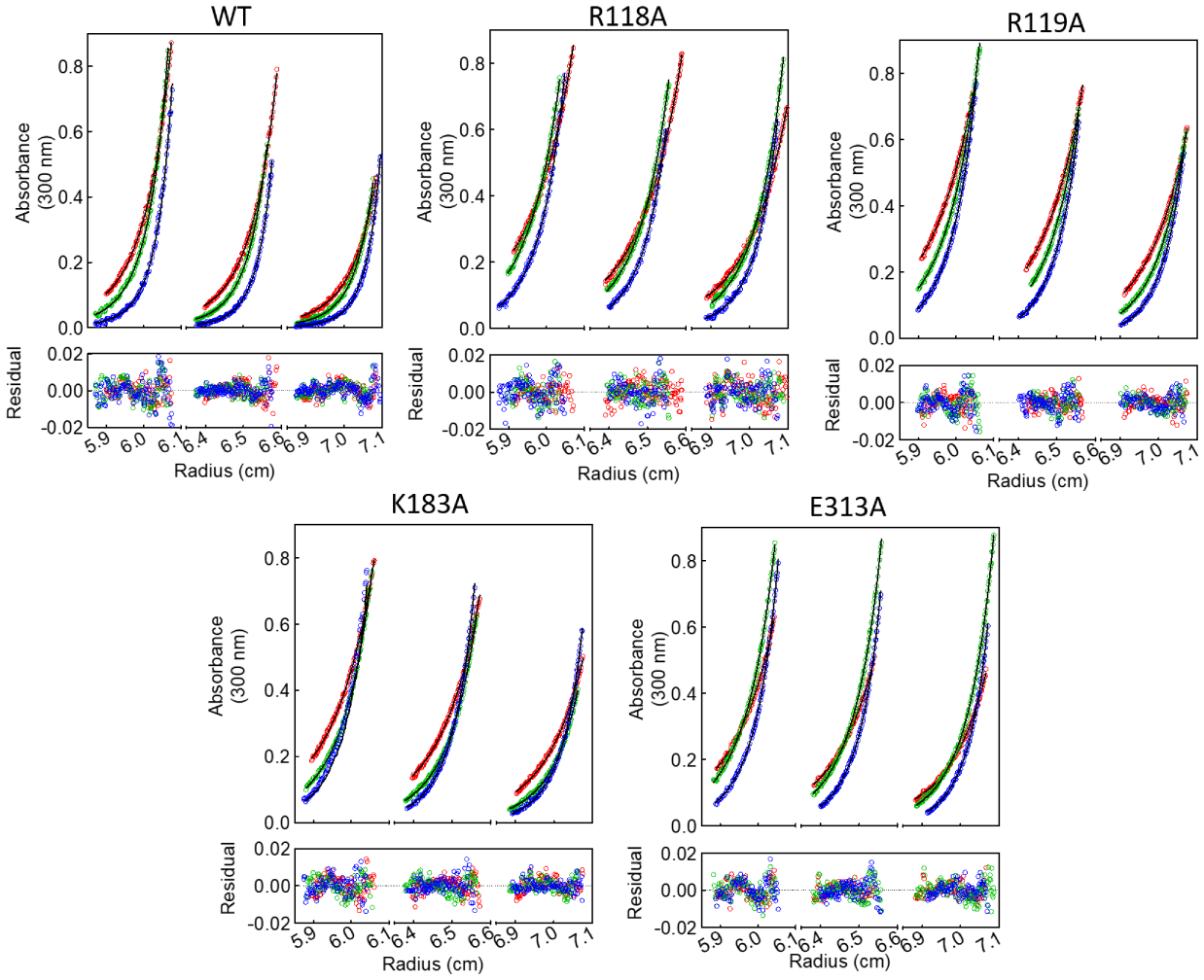

Figure S4. Absorbance versus radius profiles for holoBirA variants prepared at three loading concentrations (left> middle> right) and centrifuged at three rotor speeds. (red< green<blue). For each variant the top panel shows the data and best fit curves to a monomer-dimer association model and the bottom panel shows the residuals of the fit.

References

[1] Berendsen, H., Grigera, J., and Straatsma, T. (1987) The missing term in effective pair potentials, J Phys Chem 91, 6269-6271.

[2] Wang, J., Custer, G., Beckett, D., and Matysiak, S. (2017) Long Distance Modulation of Disorder-to-Order Transitions in Protein Allostery, Biochemistry 56, 4478-4488.

[3] Berendsen, H., van der Spoel, D., and van Drunen, R. (1995) GROMACS - A message-passing parallel molecular dynamics implementation, Comp. Phys. Comm. 91, 43-56.

[4] Lindahl, E., Hess, B., and van der Spoel, D. (2001) GROMACS 3.0: a package for molecular simulation and trajectory analysis, J. Mol. Model. 7, 306-317.

[5] Hess, B., Kutzner, C., van der Spoel, D., and Lindahl, E. (2008) GROMACS 4: Algorithms for highly efficient, load-balanced, and scalable molecular simulation, J. Chem.Theory Comput. 4, 435-447.

[6] Jorgensen, W., Maxwell, D., and TiradoRives, J. (1996) Development and testing of the OPLS all-atom force field on conformational energetics and properties of organic liquids, J. Am. Chem. Soc. 118, 11225-11236.

[7] Bussi, G., Donadio, D., and Parrinello, M. (2007) Canonical sampling through velocity rescaling, J Chem Phys 126, 014101.